

1 **Binding thermodynamics of Paromomycin, Neomycin, Neomycin-dinucleotide and -**
2 **diPNA conjugates to bacterial and human rRNA**

3

4 **Javier Alguacil, Jordi Robles*, Clara Ràfols and Elisabeth Bosch**

5

6 ¹Departament de Química Orgànica, Facultat de Química, Universitat de Barcelona

7 ²Departament de Química Analítica, Facultat de Química, Universitat de Barcelona

8 ³Institut de Biomedicina de la Universitat de Barcelona, IBUB

9 Martí i Franquès, 1-11, 08028-Barcelona, Spain

10

11 *Correspondence to: J. Robles, Departament de Química Orgànica, Facultat de Química,
12 Universitat de Barcelona, Martí i Franquès, 1-11, 08028-Barcelona, Spain.

13 E-mail: jrobles@ub.edu

14

15 J. Alguacil, J. Robles

16 Departament de Química Orgànica, Facultat de Química and Institut de Biomedicina de la
17 Universitat de Barcelona (IBUB), Universitat de Barcelona, Martí i Franquès, 1-11, 08028-
18 Barcelona, Spain.

19

20 C. Ràfols, E. Bosch

21 Departament de Química Analítica, Facultat de Química and Institut de Biomedicina de la
22 Universitat de Barcelona (IBUB), Universitat de Barcelona, Martí i Franquès, 1-11, 08028-
23 Barcelona, Spain.

24 **Abstract**

25 Isothermal titration calorimetry (ITC) is a powerful technique able to evaluate the
26 energetics of target-drug binding within the context of drug discovery. In this work the
27 interactions of RNAs reproducing bacterial and human ribosomal A-site, with two well-known
28 antibiotic aminoglycosides, Paromomycin and Neomycin, as well as several Neomycin-
29 dinucleotide and -diPNA conjugates, have been evaluated by ITC and the corresponding
30 thermodynamic quantities determined. The comparison of the thermodynamic data of
31 aminoglycosides and their chemical analogues allowed to select Neomycin-diPNA conjugates
32 as the best candidates for antimicrobial activity.

33

34 **Keywords**

35 Aminoglycosides, Antibiotics, Nucleic acids analogues, RNA, Calorimetry, Isothermal
36 Titration Calorimetry (ITC)

37 INTRODUCTION

38

39 Discovery of new drugs can be extremely helped by the thermodynamic measurements
40 of the binding interactions with biological targets by assisting high-throughput screening of
41 chemical libraries, by accelerating the lead optimization process, also for the fundamental
42 understanding of the drug-target mechanism (Ladbury *et al.*, 2010). In this context, increasing
43 improvements in the accuracy and sensitivity of instrumentation are permitting that isothermal
44 titration calorimetry (ITC) becomes the technique of choice when full thermodynamic profile
45 is valuable (Holdgate, 2007). Commonly used for proteins, until recently, ITC was applied to
46 the study of nucleic acids, and in particular, of RNA-drug complexes (Pilch *et al.*, 2003; Feig,
47 2004). An evident advantage of the technique is the simultaneous determination of the
48 thermodynamic binding constant (K_b) closely related to free energy variation (ΔG), the
49 enthalpy (ΔH) and the entropy (ΔS) variations and also the binding stoichiometry (N) from a
50 single well designed experiment (Ladbury, 2004). It should be mentioned, however, that other
51 common techniques are able to measure the ratio between the bound and free species
52 concentrations and, then, to provide the stoichiometry and the binding constant of the studied
53 interaction, but ΔH quantity cannot be directly measured. Thus, ITC seems to be the best
54 experimental approach to get a reliable and complete thermodynamic description of the
55 interaction of interest.

56 The vast knowledge acquired on RNA biochemistry, particularly, the elucidation of the
57 ribosome structure and the gene decoding at atomic level (Wimberly *et al.*, 2000; Carter *et al.*,
58 2000) has fuelled the interest on RNA-based therapies (Kole *et al.*, 2012). Similarly to proteins,
59 RNA can fold into a broad range of different structures, which can be targeted by small-
60 molecules (Aboul-ela *et al.*, 2010). In this sense, the aminoglycosides such as Paromomycin
61 and Neomycin (Fig. 1) are the paradigm of therapeutically useful RNA ligands (Hermann,

62 2005). Aminoglycosides, typically formed by an aminocyclitol unit (2-deoxystreptamine in
63 Paromomycin and Neomycin, Fig. 1) attached to one or more amino sugars via glycosidic
64 linkages, are a class of broad-spectrum antibiotics against aerobic gram-negative bacteria,
65 which exert their activity by binding to ribosomal RNA (rRNA). X-ray crystallography (Carter
66 *et al.*, 2000; Vicens and Westhof, 2001; François *et al.*, 2005) and NMR (Lynch *et al.*, 2003)
67 studies provided a very precise picture of the molecular binding mechanisms of
68 aminoglycosides. These antimicrobials target the A-site within bacterial 16S rRNA of the small
69 ribosome subunit, by binding to a three-adenine internal loop, involved in the correct
70 deciphering of the mRNA. Upon binding, aminoglycosides provoke the structural
71 rearrangement of the site, fact that eventually forge the ribosomal proofreading mechanism and
72 lead to miscoding and inhibition of protein synthesis.

73 The clinical use of aminoglycosides had been depreciated by toxicity, target
74 promiscuity and the appearance of resistance mechanisms, but the alarming decrease in the
75 activity of the current antibiotic repertoire has renewed the interest for their chemical analogues
76 (Hainrichson *et al.*, 2008). Among many other derivatives, aminoglycoside–oligonucleotide
77 conjugates have recently been considered as specific ligands of bacterial and viral RNA (Riguet
78 *et al.*, 2005; Hyun *et al.*, 2006; Charles *et al.*, 2007; Kiviniemi and Virta, 2011) due to the
79 additional chemical recognition properties conferred by oligonucleotide strands. Here, we
80 decided to contribute to this trend by developing novel aminoglycoside-oligonucleotide
81 conjugates (Alguacil *et al.*, 2010), and gaining insight on how these analogues could act as
82 specific RNA binders. We hypothesized that aminoglycosides derivatized with dinucleotide or
83 diPNA moieties could improve the target selectivity because their pending nucleobase units
84 could procure additional interactions with the RNA nucleobases close to the aminoglycoside
85 binding site by canonical or non—canonical hydrogen bonding, or by procuring complex
86 interactions as those observed in tertiary RNA motifs. As a first step, we intended to study the

87 interaction of these aminoglycoside conjugates with the validated target of aminoglycosides,
88 that is, the A-site ribosomal RNA. To this aim, inspired by the pioneer work of Pilch and col.
89 (Kaul and Pilch, 2002; Pilch *et al.*, 2003; Kaul *et al.*, 2003; Kaul *et al.*, 2005), here we present
90 the results of ITC experiments on the interaction of the aminoglycosides Paromomycin and
91 Neomycin, as well as the Neomycin-conjugates depicted in Fig. 1 with surrogates of bacterial
92 (RNA_{EC}) and human cytoplasmic rRNA (RNA_{HS}). These two 27-mer hairpin oligonucleotides
93 (Fig.2) were designed by the Puglisi group (Fourmy *et al.*, 1996; Lynch and Puglisi, 2001;
94 Lynch *et al.*, 2003) to mimic the aminoglycoside binding sites in bacterial and human rRNA,
95 respectively. The consensual bacterial target (RNA_{EC}) preferred by antibiotic aminoglycosides
96 contains an asymmetric internal loop formed by three adenines (A₁₄₀₈, A₁₄₉₂, and A₁₄₉₃,
97 according to the numbering of *Escherichia coli* rRNA sequence, Fig. 2). Instead, in the
98 eukaryotic A-site one of the adenines (A₁₄₀₈) is replaced by a guanine (G₁₄₀₈). Structural studies
99 showed that this single nucleobase change (also present in some resistant bacteria) explain why
100 human ribosomes are less sensitive to deleterious effects of aminoglycosides because reduces
101 the affinity of aminoglycosides for rRNA (Lynch and Puglisi, 2001; Kondo *et al.*, 2006).
102 Herein, we determined comparative affinities and thermodynamic values of our new analogues
103 for the bacterial *vs.* the human target, as a first step to assess their antibiotic activity and reduced
104 toxicity on humans.

105

106 **MATERIALS AND METHODS**

107

108 **Instruments**

109 Titrations were performed by means of an isothermic titration microcalorimeter
110 MicroCal VP-ITC (MicroCal, LLC, Northampton, Ma, USA) equipped with a 1.4047 mL cell.
111 A vacuum system ThermoVac, Microcal Inc. (MicroCal, LLC, Northampton, Ma, USA) was

112 used to degas the solutions. pH was measured with a Crison micro-pH 2002 potentiometer
113 (Crison Instruments, Alella, Spain) equipped by a Crison 5014 combination electrode with a
114 precision of ± 0.1 mV (± 0.002 pH units). The electrode system was standardized with ordinary
115 aqueous buffers of pH 4.01 and 7.00.

116

117 **Chemicals**

118 The two oligoribonucleotides mimicking the bacterial (RNA_{EC}) and human cytoplasm
119 (RNA_{HS}) A-site rRNA (Fourmy *et al.*, 1996; Kaul *et al.*, 2003; Kaul *et al.*, 2005) (Fig. 2) were
120 prepared by solid-phase synthesis and conveniently purified by semipreparative HPLC. The
121 compound purity has been tested by HPLC before use. Paromomycin sulfate and Neomycin
122 trisulfate (> 98%) were from Sigma-Aldrich and used as received. Neomycin-dinucleotide
123 (Neomycin-TT and Neomycin-AA) and -diPNA (Neomycin-tt and Neomycin-aa) conjugates
124 (Fig. 1) were synthesized in house as described previously (Alguacil *et al.*, 2010).

125

126 **Working solutions**

127 A mixture of sodium cacodylate 10 mM, EDTA 0.1 mM and NaCl 150 mM adjusted at
128 pH 5.5 has been used as the buffer solution. Both titrant and titrated solutions have been
129 dissolved in this buffer in all instances. For titrations involving the RNA_{EC} the concentration
130 was 10 μ M for the RNA and 200 or 300 μ M for the ligands. In the case of the RNA_{HS} titrations
131 the concentration was 20 μ M for the RNA and 500 μ M for the ligands.

132

133

134

135 **ITC measurements**

136 The RNA solutions were heated at 90°C in a sand bath and cooled down slowly, that is,
137 the sample achieves the thermal equilibrium with the ambient temperature by spontaneous
138 losing heat process until room temperature (about 20 °C). Both titrant and titrated solution were
139 deoxygenated before use. Successive volumes of 10 µL (0.5 µL s⁻¹) of ligand solution
140 (aminoglycosides, dinucleotide- or diPNA-conjugates) were added to the titration cell filled
141 with the target solution (RNA_{EC} or RNA_{HS}). At least, three independent titrations were carried
142 out for each ligand-target combination. Background titrations consisting in identical titrant
143 solutions with the reaction cell filled just with the buffer solution were performed to determine
144 the background heat, due to the ligand dilution and the syringe rotation. In all instances the
145 working temperature was 25±0.2 °C. The obtained data were analyzed through the Origin 7.0
146 software supplied by Microcal. The ITC data were collected automatically and analyzed to get
147 the N, ΔH, K_b, ΔG and ΔS values associated to the interaction. All the data have been fitted
148 with Origin and Setphat/Nitpic software. No significant differences in final results have been
149 observed using these algorithms and, then, data shown in Tables 2 and 3 are those from Origin
150 (two binding sites mode in all instances except for Neomycin_{aa}/RNA_{HS} for which the
151 sequential binding site mode has been used)

152

153 **RESULTS AND DISCUSSION**

154

155 It is well known that ITC measurements are strongly unspecific since any chemical
156 process is able to generate or consume an amount of heat. Very often, several concomitant
157 reactions are involved in interactions with biological interest and all of them can significantly
158 contribute to the measured heat (Zhang *et al.*, 2000; Garrido *et al.*, 2011). Particularly, the gain
159 or loss of protons in the frame of the global process could be relevant in the final result. Then,
160 to get biologically meaningful quantities, the experimental conditions of measurements should

161 be as close as possible to the biological environment when the interaction of interest will be
162 done.

163 Pilch and col. determined the acidity constants of protonated amino groups present in
164 Paromomycin and Neomycin and demonstrated that all of them are essentially protonated at
165 pH 5.5 (Kaul *et al.*, 2003). Therefore, the authors proposed sodium cacodylate (pH=5.5) as the
166 buffer agent for ITC titrations of RNA with Paromomycin because of the absence of ligand
167 proton exchange and, also, the very low buffer dissociation heat (Goldberg *et al.*, 2002; Kaul
168 *et al.*, 2003). Moreover, to avoid the effect of the eventual presence of metal ions traces a
169 complexing agent, EDTA, was added to the buffer solution and, also, the ionic strength was
170 adjusted to the physiological ionic concentration with NaCl. Working in this way, the derived
171 binding parameters should be as close as possible to those of the pure aminoglycoside-RNA
172 interactions. Since Paromomycin and Neomycin differ only in the 6' substituent (OH and NH₃⁺,
173 respectively), they are able to illustrate the effect of the global charge of the ligand in the
174 binding behaviour with RNA, Fig. 1.

175 As a preliminary reference, Table 1 summarizes the literature binding constants referred
176 to Paromomycin and Neomycin interactions with both RNA_{EC} and RNA_{HS} that were obtained
177 with different experimental techniques and working conditions. Overall, it is noted that
178 affinities of both aminoglycosides are higher for the bacterial RNA_{EC} than for the human target
179 and, Neomycin shows the higher binding constants for the two tested targets. Paromomycin,
180 Neomycin and the Neomycin-conjugates depicted in Fig. 1 have been selected for this study.
181 The buffer recommended by Pilch et col. (Kaul *et al.* 2003) has been also used in this work for
182 all studied aminoglycosides and conjugates under the assumption that the ammonium groups
183 of conjugates show pK_a values close enough to those of the parent compound. In addition, at
184 the selected pH the ionization of the nucleobases thymine and adenine present in conjugates
185 can be considered nearly negligible (for thymine-N3, pK_a=10.5, and for protonated adenine-

186 N1, $pK_a=3.9$; Saenger, 1984). Thus, the net charge for Paromomycin is +5, for Neomycin and
187 its diPNA conjugates it is +6, and it is +4 for Neomycin-dinucleotide conjugates.

188

189 **Aminoglycosides-RNA_{EC} interactions**

190

191 Results achieved for Paromomycin and Neomycin are summarized in Figure 3 and Table 2
192 agree with those from literature obtained in the same experimental conditions (Table 1; Kaul
193 *et al.*, 2005). Both compounds show two main interaction events and the final results are
194 consistent whichever the fitting algorithm was used. As noted previously for Paromomycin
195 (Kaul *et al.*, 2003), only this first event with the highest K_b and a stoichiometry (N_1) of
196 approximately 1 has biological relevance because it relates to the specific binding of
197 aminoglycosides to the RNA bulge site, thus it is useful for comparing affinities. The second
198 drug interaction event, with an stoichiometry (N_2) of approximately 2-3 and an affinity constant
199 (K_{b2}) two orders of magnitude lower can be ascribed to unspecific binding of aminoglycosides
200 to RNA (electrostatic and secondary interactions). This second binding event could be of
201 biological relevance when working with wild RNAs, but it is not significant enough in
202 experiments performed using small RNA surrogates, which reproduce appropriately the
203 aminoglycoside binding site only.

204 The complete thermodynamic signatures for the first binding event are depicted in Fig.
205 4. The breakdown of the overall binding affinity into its constituents values of enthalpy and
206 entropy provides useful guidelines for deducing structure-activity relationships (Ladbury *et al.*,
207 2010; Chaires, 2008). A glance on the relative magnitudes of the enthalpic, ΔH , and entropic,
208 $T\Delta S$, terms associated to the first interaction events shows the preponderance of the entropic
209 one. This result seems to contravene with the substantial binding interactions that are
210 established between the natural aminoglycosides and the bacterial A-site rRNA as shown by

211 the diffraction X-ray (François *et al.*, 2005) and NMR (Fourmy *et al.*, 1996) studies.
212 Nevertheless, this trend was characteristic for minor groove binders of nucleic acids (François
213 *et al.*, 2005). Thus, the results would be mostly explained by the structural rearrangement that
214 the aminoglycoside produces when binds into the RNA bulge which results into the
215 displacement of the adenines A1492 and A1493 to the minor groove of the helix. This provokes
216 the unstacking of the adenines which entails an enthalpy penalty. Moreover, the dependence of
217 the binding affinities on the ionic strength (Kaul and Pilch, 2002) suggests that the electrostatic
218 interactions play a significant role. Thus, since they produce the release of counterions from
219 the RNA, there is an increase of the net entropy variation. Finally, it should be pointed out that
220 target and ligand desolvation processes also alter the organized water network around both
221 entities resulting in a significant entropic gain.

222 Values gathered in Table 2 point out Neomycin as the most effective natural
223 aminoglycoside, as it binds to the RNA with higher affinity than Paromomycin (aprox. 10-fold
224 in this study, 7-fold according to Kaul *et al.*, 2006). The enhanced binding affinity of Neomycin
225 with respect to Paromomycin is clearly related to the presence of a 6'-amino instead of a
226 hydroxyl group, which results in a more favorable enthalpy.

227 With respect to conjugates, the diPNA-containing (Neomycin-tt and Neomycin-aa)
228 show K_{b1} values of the same order than the natural aminoglycoside Paromomycin but one order
229 of magnitude lower than that of Neomycin, Table 2. As diPNA-conjugates contain the same
230 number of amino groups than Neomycin, their lower affinity should be attributed to the global
231 effect of the polyamide chain. Notably, the comparison of the first event thermodynamic
232 quantities shows that the diPNA-conjugates enthalpic term is similar to that for Neomycin,
233 being higher for Neomycin-aa than for Neomycin-tt. It is well known that the formation of new
234 bonds, mainly hydrogen bonds but also van der Waals or polar interactions, favors the ΔH term.
235 Thus, an increase of enthalpy contribution points out an increment in the number and/or

236 strength of the ligand-target interactions, and probably explain the lower K_{b1} value of
237 Neomycin-aa by rapport to Neomycin-tt. By contrast, the dinucleotide-conjugates (Neomycin-
238 AA and Neomycin-TT) show a lower affinity than the diPNA-conjugates. Their enthalpic
239 contributions are significantly lower to that of the unsubstituted Neomycin, but the entropic
240 terms are similar. Thus, low affinity could be attributed either to their lower positive charge
241 with respect Neomycin and diPNA-conjugates, or to that the array of the polar groups does not
242 favor the interaction with RNA.

243

244

245 **Aminoglycosides-RNA_{HS} interactions**

246

247 The behaviour of ligands with respect the RNA_{HS}, an eukaryote target, has been also studied
248 to evaluate the selectivity, that is, the ratio between the affinities of each ligand with both
249 prokaryote and eukaryote targets. This is a key question for estimating the potential activity of
250 the compounds as antibiotics since the effectiveness as antimicrobial agents is clearly related
251 to the specificity of the rRNA-targeting molecules for the bacterial *versus* human ribosomes
252 (Kondo *et al.*, 2007). The two natural aminoglycosides as well as the diPNA-conjugates with
253 higher affinity for the bacterial target (Neomycin-tt and Neomycin-aa) have been considered
254 in this part of work. Note that K_{b1} for Paromomycin-RNA_{HS} complex in the experimental
255 conditions reported before (Table 1) is consistent with that obtained in our laboratory (Table
256 3).

257 The titration curves depicted in Fig. 5 show also, at least, two interaction steps with
258 RNA_{HS} but the shape of the ITC curves strongly differs from those obtained with the prokaryote
259 RNA_{EC}. As expected, the affinity of the aminoglycosides and the diPNA-conjugates for the
260 human target is at least one order lower than for the prokaryote target, confirming what was

261 reported for aminoglycosides and their analogues (Kaul *et al.*, 2005; Kondo *et al.*, 2007). For
262 the natural aminoglycosides, Paromomycin and Neomycin, the first event involves lower
263 enthalpic contribution than the second one despite the associated binding constant is higher
264 ($K_{b1} > K_{b2}$). Neomycin shows the highest target affinity, K_{b1} value, miming the observed
265 behaviour with the prokaryote RNA_{EC}. diPNA-conjugates show similar K_b values, close to that
266 of Paromomycin, but an order lower than Neomycin, similarly to what was observed in
267 bacterial RNA complexes. Neomycin-tt origins successive binding steps of decreasing
268 associated ΔH values. Only the two first events, the most significant ones, are included in Table
269 3. Finally, Neomycin-aa shows, at least, three interaction steps. This third event was not
270 observed in the other studied systems, and it could not be attributed any physical meaning. A
271 plausible explanation was the precipitation of RNA as a result of the saturation by positively-
272 charged aminoglycosides (a peak broadening was observed after the second binding event), but
273 any other process could be also possible. The very low RNA_{HS} concentration (20 μ M)
274 prevented to visualize any precipitation process. Then, Neomycin-aa binds RNA_{HS} in a
275 different way than other tested aminoglycosides showing a significantly higher enthalpy
276 variation. The complete thermodynamic signatures of all studied first interaction events are
277 shown in Fig. 6

278

279 **Comparison of aminoglycosides and conjugates interactions with eukaryote and** 280 **prokaryote targets**

281

282 The selectivity of aminoglycosides and conjugates for the bacterial *versus* the human RNA was
283 estimated by comparing the thermodynamic values obtained in the two sets of experiments (see
284 Tables 2 and 3). Due to the fact that binding interactions were studied on RNA surrogates of
285 wild ribosomal RNA, the thermodynamic values assigned to the second interaction were not

286 probably a robust estimation of unspecific bindings. So, in order to estimate the selectivity of
287 bacterial vs. human RNA we only considered the first interaction. At this point it should be
288 emphasized that, from the Holdgate diagram point of view (Holdgate, 2007), all the considered
289 interactions show thermodynamic parameter values with biological relevance, being all of the
290 compounds more akin to bacterial target. Notably, although Neomycin is the compound with
291 the highest selectivity for the bacterial *versus* the human RNA, diPNA-conjugates show a better
292 selectivity than Paromomycin.

293 For Paromomycin and Neomycin the differences between the two targets are, mainly,
294 of the enthalpic origin since the entropic terms are similar. The difference between the binding
295 constants is not attributable to a higher number of electrostatic interactions by Neomycin than
296 by Paromomycin since they contribute mainly to the entropic term because of the release of
297 counterions to the media (Kaul *et al.*, 2005). Then, the molecular origin of the difference in the
298 enthalpic contributions should be due to the structural differences between the two targets
299 (Lynch and Puglisi, 2001). Thus, the binding of Paromomycin to the A-site of the prokaryote
300 target origins a conformational change in the A₁₄₀₈, A₁₄₉₂ and A₁₄₉₃ residues resulting in several
301 stacking interactions which, from the energetic point of view, favour the binding process. By
302 contrast, in the eukaryote target the structure of the guanine internal loop hinders the binding
303 of the aminoglycoside.

304 Notably, according to our data, the two diPNA-conjugates show different modes of
305 binding to the RNA_{HS} target. The enthalpic term in both conjugates is higher for the eukaryote
306 target than for the prokaryote one, but the entropic term is significantly lower, Fig. 6. Then, the
307 lower affinity of the conjugated ligands to the human RNA is from an entropic origin.

308 Table 4 shows the ratio between the binding constants of the studied ligands with the
309 two targets and gives information on the selectivity of the ligands. Thus, all the tested
310 aminoglycosides show a higher preference for the prokaryote target being that of Neomycin

311 the highest one. Interestingly, the selectivities of both diPNA conjugates are similar but
312 significantly higher than for Paromomycin. In some way, this result supports the working
313 hypothesis that the derivatization of aminoglycosides with nucleobase units can improve their
314 selectivity by procuring additional interactions with RNA targets. The binding constants of
315 Paromomycin and both Neomycin derivatives with each target are similar but Neomycin-aa
316 shows a binding process mainly due to the enthalpic term whereas the remaining ligands were
317 governed by the entropy. Probably, this fact is explained by a different interaction mode of the
318 Neomycin-aa derivative, that originates in the distinctive binding properties of the pendant
319 diPNA. Notably, Neomycin-aa that shows a slightly better selectivity than Neomycin-tt, it is
320 also the aminoglycoside analogue with the highest enthalpic contribution to binding. This
321 appears to corroborate the convenience that the selection of drug candidates should be guided
322 not only by ΔG values, but also considering the $\Delta H/(T\Delta S)$ ratios because a higher enthalpic
323 term guarantees a better selectivity (Kondo *et al.*, 2007; Ladbury *et al.*, 2010).

324

325 **CONCLUSIONS**

326 Here, the comparative thermodynamic analysis by ITC of the binding interaction of
327 natural aminoglycosides and chemical analogues with A-site rRNA surrogates has permitted
328 to select Neomycin-diPNA conjugates as potential lead compounds for antimicrobial activity.
329 Although at a preliminary stage, this result seems to corroborate that it is possible to fine-tune
330 the binding of aminoglycosides to their biological targets by incorporation of ancillary
331 appendages. Work is in progress to further extend the set of aminoglycoside conjugates, and to
332 assess their potential antimicrobial activity.

333

334

335

336
337
338
339
340
341

Acknowledgement

This work was supported by funds from the Spanish Ministerio de Economía y Competitividad (Grants No. CTQ2010-19217/BQU and CTQ2010-21567-C02-01) and the Generalitat de Catalunya (2009SGR-208). J. A. acknowledges predoctoral fellowship from the University of Barcelona (BRD program).

342 **REFERENCES**

343

344 Aboul-ela F. 2010. Strategies for the design of RNA-binding small molecules. *Future Med.*
345 *Chem.* **2**: 93-119.

346 Alguacil J, Defaus S, Claudio A, Trapote A, Masides M, Robles J. 2010. A Straightforward
347 Preparation of Aminoglycoside-Dinucleotide and -diPNA Conjugates via Click Ligation
348 Assisted by Microwaves. *Eur. J. Org. Chem.* 3102-3109.

349 Carter AP, Clemons WM, Brodersen DE, Morgan-Warren RJ, Wimberly BT, Ramakrishnan
350 V. 2000. Functional insights from the structure of the 30S ribosomal subunit and its
351 interactions with antibiotics. *Nature* **407**: 340-348.

352 Chaires JB. 2008. Calorimetry and Thermodynamics in Drug Design. *Annu. Rev. Biophys.* **37**:
353 135-151.

354 Charles I, Xi H, Arya DP. 2007. Sequence-Specific Targeting of RNA with an Oligonucleotide-
355 Neomycin Conjugate. *Bioconjugate Chem.* **18**: 160-169.

356 Ennifar E, Aslam MW, Strasser P, Hoffmann G, Dumas P, van Delft FL. 2013. Structure-
357 guided discovery of a novel aminoglycoside conjugate targeting HIV-1 RNA viral genome.
358 *ACS Chem. Biol.* **8**: 2509-2517.

359 Feig AL. 2007. Applications of isothermal titration calorimetry in RNA biochemistry and
360 biophysics. *Biopolymers* **87**: 293-301.

361 Fourmy D, Recht MI, Blanchard SC, Puglisi JD. 1996. Structure of the A Site of Escherichia
362 coli 16S Ribosomal RNA Complexed with an Aminoglycoside Antibiotic. *Science* **274**:
363 1367-1371.

364 François B, Russell RJM, Murray JB, Aboul-ela F, Masquida B, Vicens Q, Westhof E. 2005.
365 Crystal structures of complexes between aminoglycosides and decoding A site

366 oligonucleotides: role of the number of rings and positive charges in the specific binding
367 leading to miscoding. *Nucleic Acids Res.* **33**: 5677-5690.

368 Garrido G, Ràfols C, Bosch E. 2011. Isothermal titration calorimetry of Ni(II) binding to
369 histidine and to *N*-2-aminoethylglycine. *Talanta* **84**: 347-354.

370 Goldberg RN, Kishore N, Lennen RN. 2002. Thermodynamic Quantities for the Ionization
371 Reactions of Buffers. *J. Phys. Chem. Ref. Data* **31**: 231-370.

372 Hainrichson M, Nudelman I, Baasov T. 2008. Designer aminoglycosides: the race to develop
373 improved antibiotics and compounds for the treatment of human genetic diseases. *Org.*
374 *Biomol. Chem.* **6**: 227-239.

375 Hermann T. 2005. Drugs targeting the ribosome. *Curr. Opin. Struct. Biol.* **15**: 355-366.

376 Holdgate GA. 2007. Thermodynamics of binding interactions in the rational drug design
377 process. *Expert Opin. Drug Discov.* **2**: 1103-1114.

378 Hyun S, Lee KH, Yu J. 2006. A strategy for the design of selective RNA binding agents.
379 Preparation and RRE RNA binding affinities of a neomycin-peptide nucleic acid
380 heteroconjugate library. *Bioorg. Med. Chem. Lett.* **16**: 4757-4759.

381 Kaul M, Pilch DS. 2002. Thermodynamics of Aminoglycoside-rRNA Recognition: The
382 Binding of Neomycin-Class Aminoglycosides to the A Site of 16S rRNA. *Biochemistry*
383 **41**: 7695-7706.

384 Kaul M, Barbieri CM, Kerrigan JE, Pilch DS. 2003. Coupling of Drug Protonation to the
385 Specific Binding of Aminoglycosides to the A Site of 16 S rRNA: Elucidation of the
386 Number of Drug Amino Groups Involved and their Identities. *J. Mol. Biol.* **326**: 1373-
387 1387.

388 Kaul M, Barbieri CM, Pilch DS. 2005. Defining the Basis for the Specificity of
389 Aminoglycoside-rRNA Recognition: A Comparative Study of Drug Binding to the A Sites
390 of *Escherichia coli* and Human rRNA. *J. Mol. Biol.* **346**: 119-134.

391 Kaul M, Barbieri CM, Pilch DS. 2006. Aminoglycoside-Induced Reduction in Nucleotide
392 Mobility at the Ribosomal RNA A-Site as a Potentially Key Determinant of Antibacterial
393 Activity. *J. Am. Chem. Soc.* **128**: 1261-1271.

394 Kiviniemi A, Virta P. 2011. Synthesis of Aminoglycoside-3'-Conjugates of 2'-O-Methyl
395 Oligoribonucleotides and Their Invasion to a ¹⁹F labeled HIV-1 TAR Model. *Bioconjugate*
396 *Chem.* **22**: 1559-1566.

397 Kole R, Krainer AR, Altman S. 2012. RNA therapeutics: beyond RNA interference and
398 antisense oligonucleotides. *Nat. Rev. Drug Discovery* **11**: 125-140.

399 Kondo J, Urzhumtsev A, Westhof E. 2006. Two conformational states in the crystal structure
400 of the Homo sapiens cytoplasmic ribosomal decoding A site. *Nucleic Acids Res.* **34**: 676-
401 685.

402 Kondo J, Hainrichson M, Nudelmanm I, Shallom-Shezifi D, Barbieri CM, Pilch DS, Westhof
403 E, Baasov T. 2007. Differential Selectivity of Natural and Synthetic Aminoglycosides
404 towards the Eukaryotic and Prokaryotic Decoding A Sites. *ChemBioChem* **8**: 1700-1709.

405 Ladbury JE, Doyle MD. 2004. *Biocalorimetry 2*. Wiley: Chichester.

406 Ladbury JE, Klebe G, Freire E. 2010. Adding calorimetric data to decision making in lead
407 discovery: a hot tip. *Nat. Rev. Drug Discov.* **9**: 23-27.

408 Lynch SR, Puglisi JD. 2001. Structure of a eukaryotic decoding region A-site RNA. *J. Mol.*
409 *Biol.* **306**: 1023-1035.

410 Lynch SR, Gonzalez RL, Puglisi JD. 2003. Comparison of X-Ray Crystal Structure of the
411 30S Subunit-Antibiotic Complex with NMR Structure of Decoding Site Oligonucleotide-
412 Paromomycin Complex. *Structure* **11**: 43-53.

413 Núñez S, Venhorst J, Kruse CG. 2012. Target–drug interactions: first principles and their
414 application to drug discovery. *Drug Discov. Today* **17**: 10-22.

415 Pilch DS, Kaul M, Barbieri CM, Kerrigan JE. 2003. Thermodynamics of Aminoglycoside–
416 rRNA Recognition, *Biopolymers* **70**: 58-79.

417 Riguet E, Désiré J, Bode O, Ludwig V, Göbel M, Baily C, Décout JL. 2005. Neamine dimers
418 targeting the HIV-1 TAR RNA. *Bioorg. Med. Chem. Lett.* **15**: 4651-4655.

419 Ryu DH, Rando RR. 2001. Aminoglycoside Binding to Human and Bacterial A-Site rRNA
420 Decoding Region Constructs. *Bioorg. Med. Chem.* **9**: 2601-2608.

421 Saenger W. 1984. *Principles of Nucleic Acid Structure*. Springer Verlag: New York.

422 Vicens Q, Westhof E. 2001. Crystal Structure of Paromomycin Docked into the Eubacterial
423 Ribosomal Decoding A Site. *Structure* **9**: 647-658.

424 Wimberly BT, Brodersen DE, Clemons WMJ, Morgan-Warren RJ, Carter AP, Vonnrhein C,
425 Hartsch T, Ramakrishnan V. 2000. Structure of the 30S ribosomal subunit. *Nature* **407**:
426 327-339.

427 Wong CH, Hendrix M, Priestley ES, Greenberg WA. 1998. Specificity of aminoglycoside
428 antibiotics for the A-site of the decoding region of ribosomal RNA. *Chem. Biol.* **5**: 397-
429 405.

430 Zhang Y, Akilesh S, Wilcox DE. 2000. Isothermal titration calorimetry of Ni(II) and Cu(II)
431 binding to His, GlyGlyHis, HisGlyHis and Bovine Serum Albumin: A critical evaluation.
432 *Inorg. Chem.* **39**: 3057-3064.

433

434 **Figure captions**

435

436 **Figure 1.** Structure of aminoglycosides (Paromomycin and Neomycin), Neomycin-
437 dinucleotide (Neomycin-TT and Neomycin-AA) and -diPNA (Neomycin-tt and Neomycin-
438 aa) conjugates.

439

440 **Figure 2.** Oligoribonucleotides mimicking the **a)** *Escherichia coli* (bacterial) A-site rRNA
441 (RNA_{EC}) and **b)** Human Cytoplasm Ribosomal A-site rRNA (RNA_{HS}). The nucleotides of the
442 internal loop are shown in bold and numbered according to the sequence of bacterial 16S
443 rRNA.

444

445 **Figure 3.** ITC curves for the interactions of Paromomycin, Neomycin and Neomycin
446 derivatives with RNA_{EC}.

447

448 **Figure 4.** Thermodynamic signatures for the interactions of Paromomycin, Neomycin and
449 Neomycin derivatives with RNA_{EC}. Color code: ΔH_1 (dark grey), $-T\Delta S_1$ (light grey), ΔG_1
450 (black).

451

452 **Figure 5.** ITC curves for the interactions of Paromomycin, Neomycin and Neomycin
453 derivatives with RNA_{HS}.

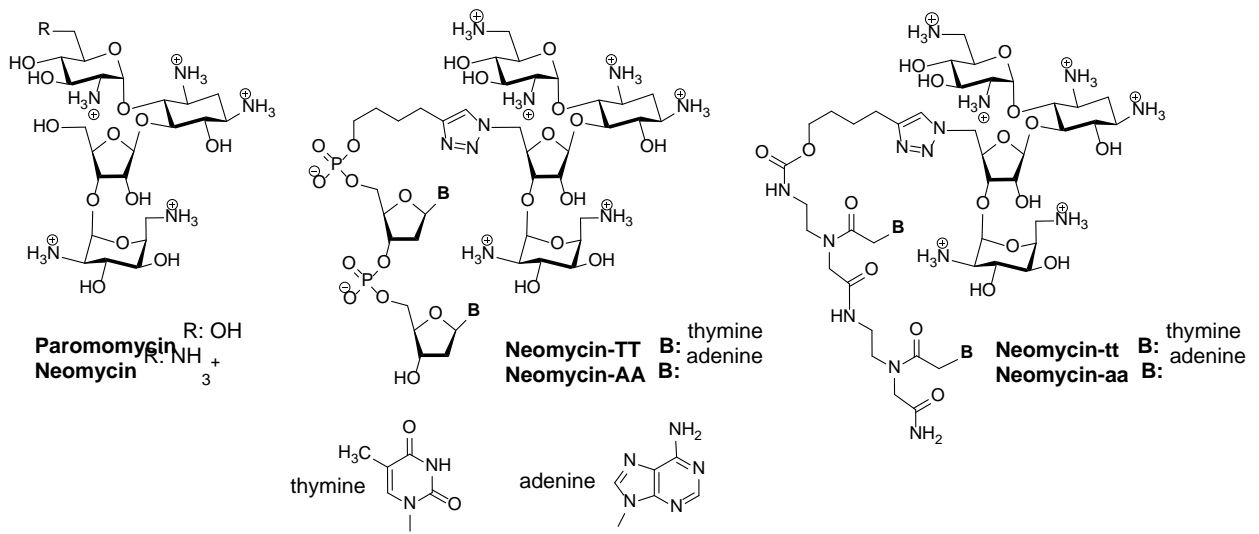
454

455 **Figure 6.** Thermodynamic signatures for the interactions of Paromomycin, Neomycin and
456 Neomycin derivatives with RNA_{HS}. Color code: ΔH_1 (dark grey), $-T\Delta S_1$ (light grey), ΔG_1
457 (black).

458

459 **Figure 1**

460

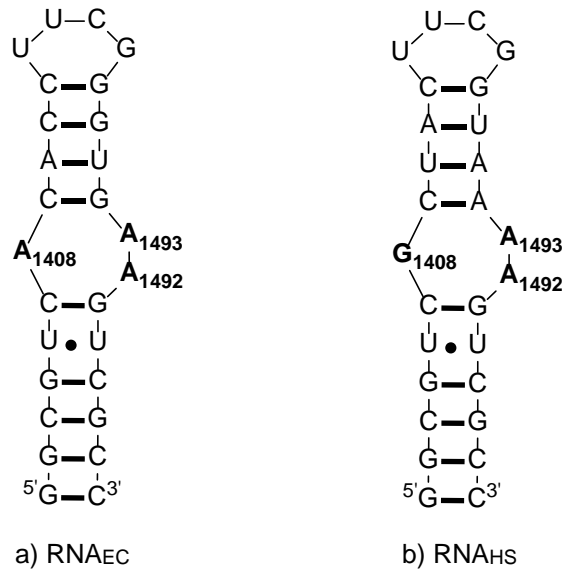


461

462

463 **Figure 2**

464



465

466

467

468 **Table 1**

469 Binding constants of the interaction of aminoglycosides with A-site rRNAs

470

Technique	K_b (M^{-1})			
	Paromomycin		Neomycin	
	Bacterial	Human	Bacterial	Human
Fluorescence	6.06×10^5 ^a	4.55×10^5 ^a	1.89×10^7 ^a	3.85×10^6 ^a
Fluorescence	2.10×10^6 ^b	3.90×10^5 ^b	3.00×10^7 ^b	---
UV-melting curves	2.50×10^7 ^c	---	2.60×10^8 ^c	---
SPR	5.00×10^6 ^d	---	5.26×10^7 ^d	---
ITC	3.70×10^7 ^e	2.40×10^6 ^e	---	---
ITC	4.34×10^6 ^f	---	4.76×10^6 ^f	---
ITC	1.27×10^5 ^g	---	1.23×10^6 ^g	---

471 ^aExperimental conditions: ^a150 mM Na⁺, pH 7.5 (Ryu *et al.*, 2001).472 ^bExperimental conditions: 100 mM Na⁺, pH 7.5 (Kaul *et al.*, 2005; Kaul *et al.*, 2006)473 ^cExperimental conditions: 150 mM Na⁺, pH 5.5 (Pilch *et al.*, 2003)474 ^dExperimental conditions: 150 mM Na⁺, pH 7.5 (Wong *et al.*, 1998)475 ^eExperimental conditions: 150 mM Na⁺, pH 5.5 (Kaul *et al.*, 2005)476 ^fExperimental conditions: 100 mM K⁺, 2 mM Mg²⁺, pH 7.0 (Ennifar *et al.*, 2013)477 ^gExperimental conditions: 200 mM K⁺, 2 mM Mg²⁺, pH 7.0 (Ennifar *et al.*, 2013)

478

479

480

481 **Table 2**482 Binding parameters of the studied ligands with RNA_{EC}

483

	Paromomycin	Neomycin	Neomycin-TT	Neomycin-AA	Neomycin-tt	Neomycin-aa
N_1	1.1 ± 0.1	1.0 ± 0.1	1.0 ± 0.1	0.9 ± 0.0	0.8 ± 0.1	0.8 ± 0.0
K_{b1} (M^{-1})	(1.7 ± 0.2) $\times 10^7$	(2.1 ± 0.7) $\times 10^8$	(1.3 ± 0.3) $\times 10^7$	(2.2 ± 0.7) $\times 10^6$	(5.7 ± 1.1) $\times 10^7$	(3.4 ± 2.0) $\times 10^7$
ΔG_1 ($kcal \cdot mol^{-1}$)	-9.9 ± 0.2	-11.4 ± 0.2	-10.0 ± 0.1	-8.6 ± 0.2	-10.6 ± 0.1	-10.2 ± 0.3
ΔH_1 ($kcal \cdot mol^{-1}$)	-3.1 ± 0.3	-5.4 ± 0.0	-2.8 ± 0.4	-3.4 ± 0.0	-4.1 ± 0.2	-6.2 ± 0.2
$-T\Delta S_1$ ($kcal \cdot mol^{-1}$)	-6.7 ± 0.3	-6.0 ± 0.1	-6.9 ± 0.3	-5.2 ± 0.2	-6.5 ± 0.3	-4.0 ± 0.6
N_2	3.0 ± 0.5	3.0 ± 0.1	2.0 ± 0.8	2.6 ± 0.4	3.1 ± 0.1	2.6 ± 0.0
K_{b2} (M^{-1})	(3.0 ± 0.5) $\times 10^5$	(7.6 ± 0.7) $\times 10^5$	(8.2 ± 0.8) $\times 10^5$	(1.2 ± 0.4) $\times 10^5$	(2.3 ± 0.7) $\times 10^5$	(2.0 ± 0.0) $\times 10^5$
ΔG_2 ($kcal \cdot mol^{-1}$)	-7.5 ± 0.0	-8.0 ± 0.0	-8.1 ± 0.0	-6.9 ± 0.2	-7.3 ± 0.2	-7.2 ± 0.0
ΔH_2 ($kcal \cdot mol^{-1}$)	-2.1 ± 0.5	-4.5 ± 0.3	-0.8 ± 0.6	-1.0 ± 0.4	-4.5 ± 0.3	-6.6 ± 0.1
$-T\Delta S_2$ ($kcal \cdot mol^{-1}$)	-5.4 ± 0.6	-3.5 ± 0.4	-7.3 ± 0.6	-5.9 ± 0.2	-2.8 ± 0.4	-0.6 ± 0.1

Experimental conditions: 10 mM sodium cacodylate, 0.1 mM EDTA, 150 mM NaCl, pH 5.5, 25 ± 0.2 °C

484

485

486

487 **Table 3**488 Binding parameters of the studied ligands with RNA_{HS}

489

	Paromomycin ^a	Neomycin ^a	Neomycin-tt ^a	Neomycin-aa ^{a,b}
N ₁	1.5 ± 0.2	1.3 ± 0.0	1.2 ± 0.1	---
K _{b1} (M ⁻¹)	(5.2 ± 2.1) × 10 ⁶	(1.7 ± 0.2) × 10 ⁷	(7.3 ± 3.0) × 10 ⁶	(3.7 ± 1.8) × 10 ⁶
ΔG ₁ (kcal·mol ⁻¹)	-9.1 ± 0.2	-9.9 ± 0.0	-9.3 ± 0.3	-8.9 ± 0.3
ΔH ₁ (kcal·mol ⁻¹)	-0.6 ± 0.3	-2.7 ± 0.0	-4.9 ± 0.1	-7.3 ± 0.0
-TΔS ₁ (kcal·mol ⁻¹)	-8.5 ± 0.5	-7.2 ± 0.0	-4.4 ± 0.3	-1.6 ± 0.3
N ₂	2.3 ± 0.7	2.1 ± 0.1	2.8 ± 0.1	---
K _{b2} (M ⁻¹)	(8.2 ± 1.6) × 10 ⁵	(1.7 ± 0.2) × 10 ⁵	(1.1 ± 0.0) × 10 ⁵	(9.5 ± 2.4) × 10 ⁵
ΔG ₂ (kcal·mol ⁻¹)	-6.7 ± 0.2	-7.1 ± 0.0	-6.9 ± 0.0	-8.1 ± 0.2
ΔH ₂ (kcal·mol ⁻¹)	-2.2 ± 0.3	-5.3 ± 0.2	-5.0 ± 0.2	-4.0 ± 0.0
-TΔS ₂ (kcal·mol ⁻¹)	-4.5 ± 0.4	-1.9 ± 0.3	-1.8 ± 0.3	-4.1 ± 0.2

^aExperimental conditions: 10 mM sodium cacodylate, 0.1 mM EDTA, 150 mM NaCl, pH 5.5, 25 ± 0.2 °C

^bIn this case, curves could be only adjusted to a sequential binding mode, up to a total of three calorimetric events.

490

491

492

493 **Table 4**

494 Estimation of selectivity for RNA_{EC} vs RNA_{HS} (K_{b1} ratios)

495

	Paromomycin	Neomycin	Neomycin-tt	Neomycin-aa
$K_{b1}(\text{RNA}_{\text{EC}})/K_{b1}(\text{RNA}_{\text{HS}})$	3	12	8	9

496